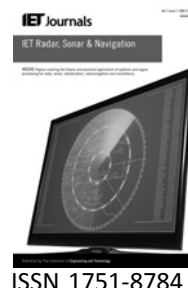


Published in IET Radar, Sonar and Navigation  
 Received on 11th March 2008  
 Revised on 25th September 2008  
 doi: 10.1049/iet-rsn:20080106



# Orthogonal frequency-division multiplexing radar signal design with optimised ambiguity function and low peak-to-average power ratio

M.A. Sebt A. Sheikhi M.M. Nayebi

Department of Electrical Engineering, Sharif University of Technology, Azadi Ave., PO Box 11365-9363, Tehran, Iran  
 E-mail: ma\_sebt@ee.sharif.edu

**Abstract:** Considering the important role of the ambiguity function (AF) of a signal regarding the performance of a matched filter bank for the detection of targets and the estimation of their ranges and velocities, the thumbtack shape is assumed to be the desirable shape of the AF and the method of least squares for the synthesis of the AF is introduced. Then, an iterative method for the allocation of a proper phase to the desired AF is proposed to obtain better results. This method is then applied to select the proper codes for the synthesis of pulsed orthogonal frequency-division multiplexing signals. It is also shown how this method can reduce sidelobes, almost uniformly, throughout the entire ambiguity plane. Finally, an efficient algorithm is presented, which modifies the produced codes in order to reach a lower peak-to-average power ratio suitable for transmission.

## 1 Introduction

In most radar systems, it is desirable to have very good resolution both in the range and Doppler domain. Over the past several decades, many methods have been invented to achieve this goal. Perhaps the first suggestion to improve range resolution was to use pulses with very short time durations. Of course, it is possible to achieve high resolution in the range domain with such a pulse, but when the pulse length is small, Doppler resolution and the energy per pulse will be really poor [1]. As a result, some authors have developed long-duration pulses with such a structure that high resolutions can be achieved in both the range and Doppler domains. Perhaps the most famous signal with this characteristic is associated with the Barker codes. A nearly complete list of such signals can be found in [2].

In signals designed with the Barker codes, a single-carrier frequency is used and the phase of this sinusoid is changed according to the code. This method has two problems. First, considering the problem of minimum detectable range, the duration of each chip should be short enough and, thus, it is difficult to implement such a system. Besides, since the spectrum of the Barker phase coded

signal is almost similar to the sinc function, the bandwidth efficiency is low [3]. Because of these problems, some other signalling schemes are needed with good range–Doppler properties, but not very short chip lengths.

One family of pulses with the so-called property was developed by Costas [4] and its recently improved version was introduced in [5]. The Costas signals have very good range–Doppler properties. The chip length is not very small, but each chip contains only one frequency, which is not favourable considering the low probability of intercept (LPI) requirements.

Another family of signals, which can achieve high resolution in both the delay and Doppler domain without the reduction of the chip duration, are the orthogonal frequency-division multiplexing (OFDM) radar signals that have been mainly investigated by Levanon [3, 5–9]. The pulsed form of this type of signal has the following general structure for each pulse

$$S(t) = \sum_{n=1}^N \sum_{m=1}^M a_{n,m} \exp\left(j \frac{2\pi(n-1)t}{t_b}\right) P(t - (m-1)t_b) \quad (1)$$

Here,  $P(t)$  is a rectangular pulse with a duration equal to  $t_b$ , and the total duration of  $S(t)$  is  $T = Mt_b$ . We name the coefficients  $a_{n,m}$  the  $N \times M$  code, and they should be determined such that the signal can have an ambiguity function (AF) with a narrow mainlobe and low sidelobes. This type of signal has a range resolution of  $t_b/N$  and a Doppler resolution of  $1/Mt_b$  [6], and can be easily produced [10] and quickly processed [11]. Levanon has used the concept of complementary sets [12, 13] to find these coefficients. In his papers, the AF is optimised only along the zero-Doppler axis. However, for applications in which both the target range and velocity are expected to be computed by each pulse, it is favourable to reduce the sidelobe levels everywhere in the Doppler–Delay plane. This type of optimisation (by proper choice of  $a_{k,l}$ ) is the main goal of our paper.

For optimisation, we have selected the method of AF synthesis; for this purpose, there are many valuable papers [14–18] that have proposed methods for the synthesis of AF. For example, in [14], AF synthesis has been implemented via burst-pulse time-frequency coding. However, in that paper, a large time-bandwidth is required for the proposed method to work well, which is neither desirable nor suitable for the OFDM signals that we have in mind. Another method is proposed in [15]. In this paper, the problem of constructing a waveform with globally optimal ambiguity surface properties in a region surrounding the mainlobe has been considered. The problem has been solved by the hermite waveform as the basis function, but the drawback here is that the implementation of the hermite function in practice is not so easy, and this type of waveform is not easily compatible with the form of the signal represented by (1). In [16], the Zak transform has been used for synthesis, but as numerical calculations show, the matrix of coefficients ( $[a_{n,m}]_{N \times M}$ ) obtained by this technique has one dominant non-zero element in each row, and therefore the small components of the matrix of coefficients can be neglected, which effectively makes it a matrix with only one non-zero element in each row. This makes the waveform a frequency hop signal, which is not suitable regarding LPI characteristics. The most effective method of synthesis on which our approach is based was introduced in [17, 18] and described in Section 2.

In Section 3, we develop the proposed method for the synthesis of the pulsed OFDM signal and extract the required equations to achieve the desired AF. In Section 4, some results are presented to evaluate the proposed method of synthesis. In Section 5, the problem of a non-constant signal envelope is explained and an algorithm to overcome this problem is presented in which, by refining the codes, one can efficiently reduce the peak-to-average power ratio (PAPR). Then, in Section 6, the algorithm is applied to refine the code obtained in Section 5. Following discussions, in Section 7, a conclusion is drawn.

## 2 Least-squares synthesis of AF

In this method, the transmitted radar signal is assumed to be a summation of some orthonormal signals named basis functions

$$u(t) = \sum_{i=1}^R a_i \phi_i(t) \quad (2)$$

where  $R$  is the number of orthonormal bases. The cross AF of these signals is defined as

$$K_{k,l}(\tau, \nu) = \int \phi_k\left(t - \frac{\tau}{2}\right) \exp(-j2\pi\nu t) \phi_l^*\left(t + \frac{\tau}{2}\right) dt \quad (3)$$

It is easy to prove that  $\{K_{k,l}(\tau, \nu)\}_{k,l=1}^R$  is an orthonormal set. The total AF of the signal  $[u(t)]$  can be expressed as

$$\chi(\tau, \nu) = \sum_{k,l} a_k a_l^* K_{k,l}(\tau, \nu) \quad (4)$$

The desired AF is  $F(\tau, \nu)$ , and we want to minimise the error which is defined as

$$\varepsilon = \iint |F(\tau, \nu) - \chi(\tau, \nu)|^2 d\tau d\nu \quad (5)$$

Referring to (4), the error can be written as

$$\varepsilon = \|F\|^2 + \sum_{k,l} |a_k a_l^*|^2 - \sum_{k,l} a_k a_l^* \langle K_{k,l}, F \rangle - \sum_{k,l} a_k^* a_l \langle F, K_{k,l} \rangle \quad (6)$$

Here,  $\langle \cdot, \cdot \rangle$  represents the inner product of the functions. Defining the elements of matrix  $\mathbf{B}$  as the inner products of  $F$  and  $K_{k,l}$

$$B_{k,l} = \langle F, K_{k,l} \rangle = \iint F(\tau, \nu) K_{k,l}^*(\tau, \nu) d\tau d\nu \quad (7)$$

The error can be expressed as

$$\varepsilon = \|F\|^2 + (\mathbf{a}^H \mathbf{a})^2 - \mathbf{a}^H (\mathbf{B} + \mathbf{B}^H) \mathbf{a} \quad (8)$$

Here,  $\mathbf{a}$  is the vector of coefficients ( $a_i$ ) and the notation  $H$  stands for the transpose conjugate. To minimise the error, the derivative of the above equation, with respect to vector  $\mathbf{a}$ , should be equated to zero. This results in the following equation

$$(\mathbf{B} + \mathbf{B}^H) \mathbf{a} = 2E \mathbf{a} \quad (9)$$

where  $E$  is defined as

$$E = \mathbf{a}^H \mathbf{a} = \sum_i a_i^2 \quad (10)$$

Therefore  $\mathbf{a}$  should be equal to one of the eigenvectors of  $\mathbf{B}$ . If the vector  $\mathbf{a}$  satisfies this condition, the error can be expressed as

$$\varepsilon = \|F\|^2 - E^2 \quad (11)$$

Therefore  $\mathbf{a}$  should be the eigenvector of matrix  $\mathbf{B}$  corresponding to the eigenvalue, which has a maximum absolute value.

Since only the magnitude of  $F(\tau, \nu)$  is of interest, by allocating the proper phase to  $F(\tau, \nu)$ , the error introduced in (11) can be reduced. Hence, the phase-matching process to improve the shape of the obtained AF is used. The description of this method follows.

For clarity, first, we consider the Hermitian case for  $F^{(0)}(\tau, \nu)$  (unmodified first desired AF). This means

$$F^{(0)}(\tau, \nu) = F^{(0)*}(-\tau, -\nu) \quad (12)$$

Hence, as mentioned before, we have

$$F^{(0)}(\tau, \nu) \simeq \sum_{k,l=1}^R B_{k,l}^{(0)} K_{k,l}^{(0)}(\tau, \nu) \quad (13)$$

According to  $B_{k,l}^{(0)} = \langle F^{(0)}(\tau, \nu), K_{k,l}^{(0)}(\tau, \nu) \rangle$ , it is clear that the matrix  $\mathbf{B}^{(0)}$  is also Hermitian and by a unitary transform  $\mathbf{Q}^{(0)}$ , we have

$$\mathbf{Q}^{(0)H} \mathbf{B}^{(0)} \mathbf{Q}^{(0)} = \mathbf{\Lambda}^{(0)} = \begin{bmatrix} \lambda_1^{(0)} & 0 & \dots & 0 \\ 0 & \lambda_2^{(0)} & 0 & \vdots \\ \vdots & 0 & \ddots & 0 \\ 0 & \dots & 0 & \lambda_R^{(0)} \end{bmatrix} \quad (14)$$

Now, we define  $K_{k,l}^{(1)}(\tau, \nu)$  as follows

$$\underline{K}^{(1)*}(\tau, \nu) = \mathbf{Q}^{(0)H} \underline{K}^{(0)*}(\tau, \nu) \mathbf{Q}^{(0)} \quad (15)$$

where  $\underline{K}^{(i)}(\tau, \nu)$  is the matrix of  $[K_{k,l}^{(i)}(\tau, \nu)]_{R \times R}$ .  $\{K_{k,l}^{(1)}(\tau, \nu)\}_{k,l=1}^R$  is an orthonormal set of bases and according to (14) and (13), we have

$$F^{(0)}(\tau, \nu) \simeq \sum_{n=1}^R \lambda_n^{(0)} K_{n,n}^{(1)}(\tau, \nu) \quad (16)$$

Then, among  $K_{i,i}^{(1)}(\tau, \nu) (i = 1, 2, \dots, R)$ , the one for which the following expression has the maximum value is chosen

$$B_{b,b}^{(1)} = \frac{1}{2\pi} \int \int |F^{(0)}(\tau, \nu)| |K_{b,b}^{(1)}(\tau, \nu)| d\tau d\nu \quad (17)$$

Now, we have

$$K_{b,b}^{(1)*}(\tau, \nu) = |K_{b,b}^{(1)}(\tau, \nu)| e^{-j\phi_{b,b}^{(1)}(\tau, \nu)} \quad (18)$$

where  $|K_{b,b}^{(1)}(\tau, \nu)|$  and  $\phi_{b,b}^{(1)}(\tau, \nu)$  are the modulus and argument of  $K_{b,b}^{(1)}(\tau, \nu)$ , respectively. We will define

$$F^{(1)}(\tau, \nu) = |F^{(0)}(\tau, \nu)| e^{j\phi_{b,b}^{(1)}(\tau, \nu)} \quad (19)$$

It can be shown that  $F^{(1)}(\tau, \nu)$  leads to less error compared with  $F^{(0)}(\tau, \nu)$ . For proof, it is sufficient to note that according to (17) and (18),  $B_{b,b}^{(1)} \geq \max_n \lambda_n^{(0)}$  and  $\varepsilon^{(1)} = \|F(\tau, \nu) - B_{b,b}^{(1)} K_{b,b}^{(1)}(\tau, \nu)\|^2 = \|F(\tau, \nu)\|^2 - |B_{b,b}^{(1)}|^2$ , but we know that  $\min \varepsilon^{(1)} = \|F(\tau, \nu)\|^2 - \lambda_{\max}^{(1)^2}$ , so  $\lambda_{\max}^{(1)^2} \geq \lambda_{\max}^{(0)^2}$ , and this completes the proof. If we continue the above procedure, the algorithm will converge to the allocation of the best phase.

### 3 Using AF synthesis method to optimise OFDM signal

We define the elements of the OFDM signal as

$$\begin{aligned} \phi_i(t) &= \phi_{qM+r}(t) = \exp\left(j2\pi\left(q - \frac{N-1}{2}\right)\frac{t}{t_b}\right) \times P(t - rt_b) \\ 0 &\leq q \leq N-1 \\ 0 &\leq r \leq M-1 \\ 0 &\leq i = qM + r \leq MN-1 \end{aligned} \quad (20)$$

This means that the signal contains  $M$  chips, each containing  $N$  different carrier frequencies. Such a constellation is shown in Fig. 1.

The cross AF of these functions is defined as (3). It is easy to show that for the signals defined by (20), the cross AF is

$$\begin{aligned} K_{k,l}(\tau, \nu) &= \begin{cases} \frac{1}{t_b} \exp\left(-j\pi\frac{\tau}{t_b} + j\pi(N-1)\tau_b\right) \\ \times \text{sinc}\left((f_b + \frac{\Delta}{q})\left(1 - \left|\tau_b - \frac{\Delta}{r}\right|\right)\right) & \left|\tau_b - \frac{\Delta}{r}\right| \leq 1 \\ \times \left(1 - \left|\tau_b - \frac{\Delta}{r}\right|\right) & \\ 0 & \text{otherwise} \end{cases} \end{aligned} \quad (21)$$

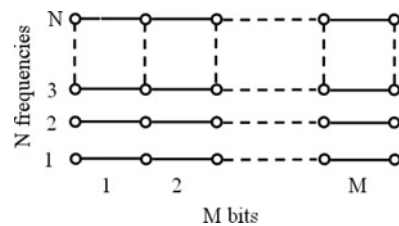


Figure 1 OFDM signal schematic representation

in which

$$\begin{aligned} k &= q_1 M + r_1, \quad l = q_2 M + r_2, \quad \tau_b = \frac{\tau}{t_b}, f_b = v t_b, \\ \bar{q} &= q_1 + q_2, \quad \bar{q} = q_2 - q_1, \quad \bar{r} = r_2 - r_1 \end{aligned} \quad (22)$$

Also, it is clear that all  $\phi_i(t)$  in (20) are orthogonal. As a result, the  $K_{k,l}(\tau, v)$  functions are orthogonal and the method given in Section 2 is applicable for the optimisation of this problem. According to this method, we should first select a desired AF. In this paper, the following AF is selected for optimisation

$$F(\tau, v) = \begin{cases} 1 & -\frac{1}{Mt_b} < v < \frac{1}{Mt_b} - \frac{t_b}{N} < \tau < \frac{t_b}{N} \\ \alpha & \text{otherwise} \end{cases} \quad (23)$$

where  $\alpha$  is the sidelobe level with a value in the range of (0,1). It should be mentioned that, according to [3], with  $M$  chips and  $N$  different frequencies, no better resolution than that explained in the above equation is achievable. Besides, it is very important to remember that according to this method, the sidelobes of ideal AF should not be equal to zero, as otherwise, the method will attempt to minimise the overall energy in the sidelobes, which is always constant, and any peak in the sidelobes will be ignored. Therefore the sidelobes of the ideal AF should be considered greater than zero. However, the value of  $\alpha$  in the above equation should be practically determined (e.g.  $\alpha = 0.1$ ).

Using computer simulation, all the calculations should be done in a discrete manner. Therefore it is necessary to find the discrete-time counterparts of (2)–(4). First, we have

$$\begin{aligned} \phi_i[n] &= \exp\left(j \frac{2\pi}{L} q n\right) P_d[n - rL] \\ i &= qM + r \\ 0 &\leq q \leq N - 1 \\ 0 &\leq r \leq M - 1 \end{aligned} \quad (24)$$

where  $P_d[\cdot]$  is a discrete pulse of length  $L$ . It is important to select the parameter  $L$  in the above equation in order to maintain the orthogonality of the functions. One choice for such a situation is  $L = N$ . By this choice ( $L = N$ ), since only one sample of the mainlobe of the desired AF appears in the simulation, the difference between the levels of the mainlobe and sidelobe does not influence the simulation results. Hence, choosing any non-zero  $\alpha$  will lead to the same results. Accepting this value, the cross AFs will be

$$\begin{aligned} K_{k,l}[m, n] &= \exp\left(-j \frac{2\pi}{L} q_2 m - j \pi \frac{nm}{LM}\right) \\ &\times H\left(m, \{-n + M \frac{\Delta}{q}\}_{ML}\right) \end{aligned} \quad (25)$$

in which

$$H(m, n) = \begin{cases} \exp(j(\pi n/ML)) \\ [( \frac{\Delta}{r} + 1)L - m - 1]) \\ \sin((\pi n/ML)) \\ \times \frac{(l - |m - \frac{\Delta}{r} L|)}{\sin(\pi n/ML)}, & |m - \frac{\Delta}{r} L| \leq L - 1 \\ 0 & \text{otherwise} \end{cases} \quad (26)$$

The following properties can be easily proved about the above-mentioned functions

$$\begin{aligned} \sum_{n=0}^{ML} \phi_i[n] \phi_j^*[n] &= L \delta(i - j) \\ K_{i,j}^*[m, n] &= K_{j,i}[-m, -n] \\ \sum_m \sum_n K_{i,j}[m, n] K_{l,r}^*[m, n] &= ML^3 \delta(i - l) \delta(j - r) \end{aligned} \quad (27)$$

Therefore these functions have all the necessary conditions of the Sussman algorithm [18], and the methods mentioned in the previous section are directly applicable.

## 4 Simulation results of AF optimisation

In this section, we have simulated the method of the previous section to find the optimum coefficients of the signal of (1). Here, the signal consists of seven chips ( $M = 7$ ) and seven orthogonal carriers ( $N = 7$ ). The result of optimisation without phase matching is presented in Fig. 2. As it is shown, the sidelobes are almost minor along the zero-Doppler axis, but the situation is not so favourable along the other axis. In this figure, the energy of the sidelobes is concentrated along the zero delay axis. This phenomenon

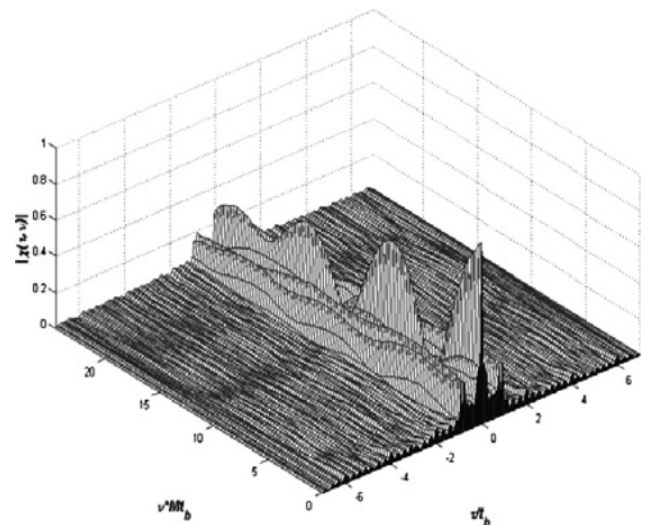


Figure 2 AF without phase matching ( $M = 7$ ,  $N = 7$ )

**Table 1** Designed code parameters

Freq	Bit						
	1	2	3	4	5	6	7
(a) Magnitude							
1	4	3	2	1	3	3	16
2	19	9	1	8	1	2	27
3	16	9	21	17	20	20	12
4	31	17	4	4	4	5	16
5	31	17	4	4	4	5	16
6	16	9	21	17	20	20	12
7	19	9	1	8	1	2	27
(b) Phase (degree)							
1	−115	−115	65	65	65	−115	65
2	60	158	179	−180	58	138	109
3	145	−90	−106	−77	−86	−89	98
4	130	60	−116	37	−58	91	−102
5	0	71	−113	94	−172	39	−128
6	−15	−140	−123	−152	−144	−140	33
7	70	−27	−48	−50	72	−8	21

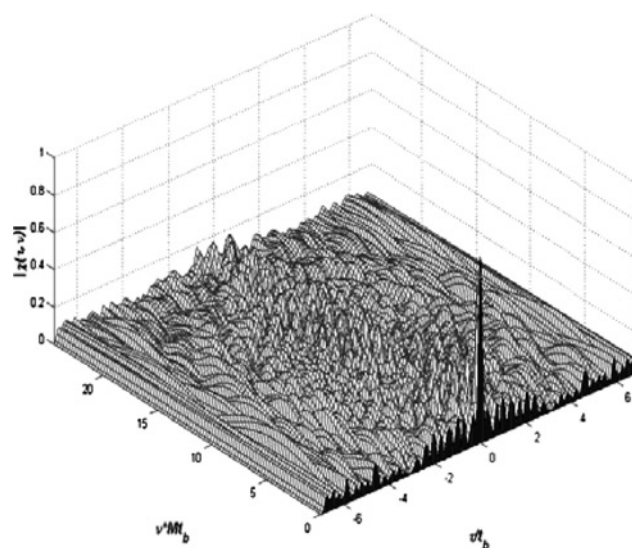
has created strong sidelobes and therefore it is necessary to use phase matching in order to achieve better results. The obtained code after phase matching is presented in Table 1 and the resultant AF is shown in Fig. 3. In this figure, the method of phase matching is used for 20 iterations. As it is shown, the sidelobes are reduced everywhere and the energy of the sidelobes is distributed almost uniformly. Here, the difference between the mainlobe and sidelobe levels is more than 10 dB all across the Doppler–delay plane (the latter being below the former).

As was shown in Section 2, the difference between the desired AF and the result of optimisation is inversely proportional to the maximum eigenvalue of the matrix of coefficients (i.e.  $\mathbf{B}$ ). Therefore the maximum eigenvalue can be considered as the termination rule in the phase-matching iterative method.

In Fig. 4, the values of the maximum eigenvalue are plotted for several iterations. Referring to this figure, after 15–20 iterations, the maximum eigenvalue has become almost constant. This means that more iterations have no significant effect on sidelobe reduction. However, contrary to the optimum behaviour of the AF, as shown in Figs. 5a and 5b, the PAPR and auto-correlation function sidelobe level (ACF SLL) are both high (PAPR = 7.7, ACF SLL = −15 dB). Therefore in the next section, a method is proposed to improve these parameters.

## 5 Code modification for PAPR reduction

One of the major drawbacks of multi-frequency signals such as OFDM is their high PAPR, which is observable for the signal corresponding to the code of Table 1 as shown in Fig. 5b. In fact, a varying amplitude signal needs the transmitter to work in its linear operating region where the

**Figure 3** AF after 20 iterations



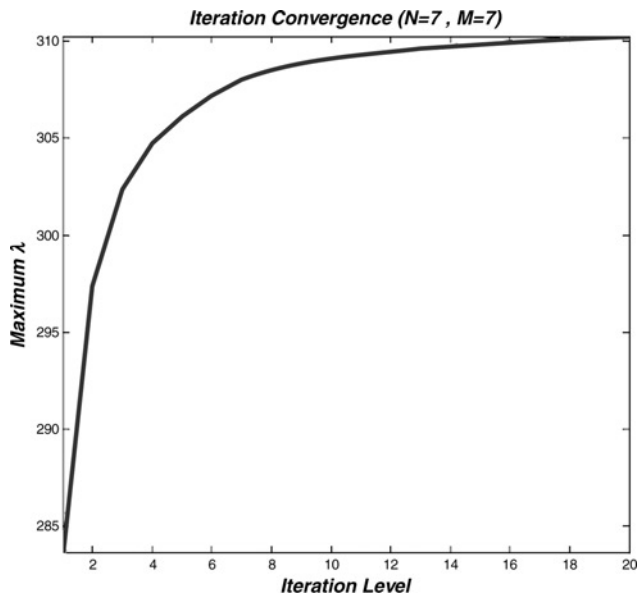


**Figure 4** Iteration convergence ( $N = 7$ ,  $M = 7$ )

power conversion is inefficient. This may have deleterious effects on transmitter lifetime. A new version of the OFDM signal for radar application has recently been proposed, which has a constant envelope [19], but this type of signal loses some of the advantages of typical OFDM signals such as bandwidth efficiency. Hence, it is very important to look for some proper methods through which it would be possible to reduce the PAPR of the OFDM signal. There are many such methods, and for more in-depth treatment, the reader is referred to a review by Han and Lee [20]. All the methods presented in [20] change the signal waveform regardless of its AF and ACF. In fact,

the important feature in these methods is the reduction of the PAPR along with the preservation of information. However, in our application, no information is taken into consideration, and the important factor is the low sidelobes in AF and ACF that will be corrupted by these methods. For radar applications, there are many valuable papers in which techniques are presented, which can lead to multi-frequency signals with a low level of the PAPR. Some of them [21–24] introduce initial phase schemes in a closed form for each tone of a multi-frequency signal. However, these methods are not suitable for our work since the phases and amplitudes of the tones in our OFDM signal are determined by the AF optimisation algorithm and the sole purpose of their modification is to obtain a low PAPR signal; changing them without any ACF or AF consideration is undesirable. There are also some other valuable papers [25–28] that present algorithms for the refinement of the phases of harmonics to achieve lower PAPR. However, these methods also do not take into account the AF and ACF. An algorithm will be introduced here in which by modifying both phases and amplitudes of codes the PAPR can be reduced more powerfully. Another method that is applicable for radar signals is proposed in [9]. In that paper, the authors have utilised the linear carrier phase shift idea and the clipping method of [25] to reduce the PAPR. That method is applied with one parameter of optimisation and is for identically sequences multi-carrier phase coded signals; however, but here we have expanded and generalised this technique to the general pulsed OFDM of (1).

Before the explanation of the algorithm, we should emphasise that because our proposed method only modifies the codes (obtained from Section 3 or any other code), it

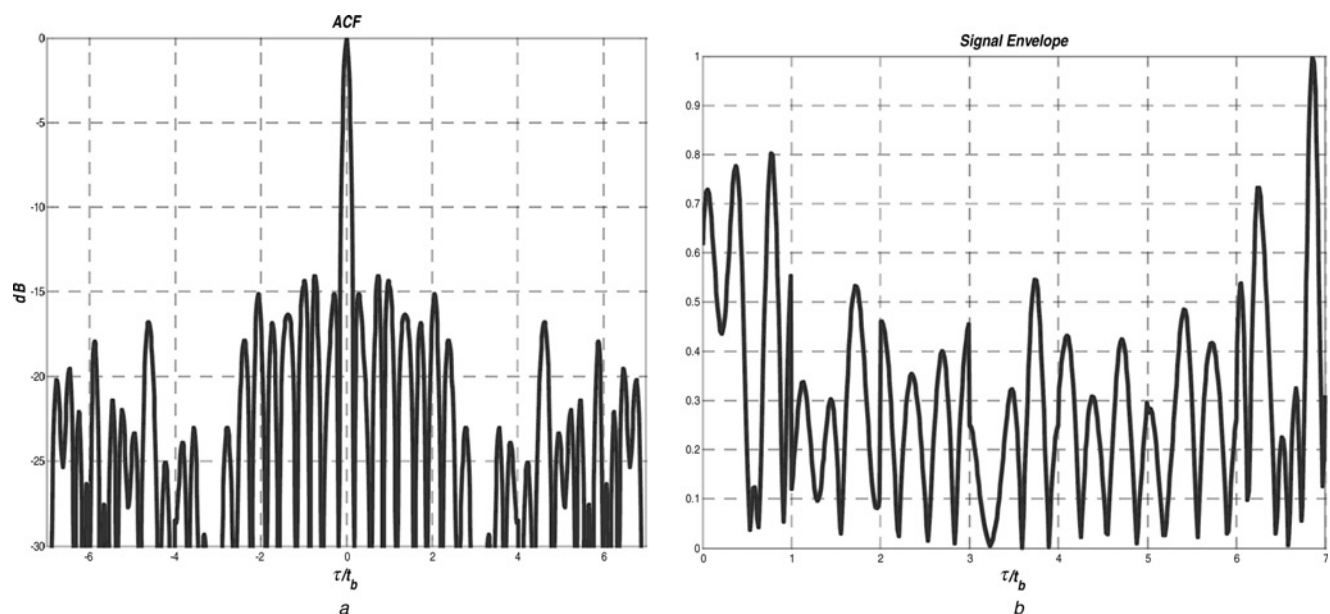


**Figure 5** ACF of the designed OFDM signal and real envelope of the designed OFDM signal

a ACF of the designed OFDM signal  
b Real envelope of the designed OFDM signal

does not require any additional hardware equipment such as a limiter.

Now, we introduce the parameter of PAPR. For a multi-frequency signal such as (1), the PAPR is defined as

$$\text{PAPR} = \frac{\max_{0 \leq t < Mt_b} |S(t)|^2}{(1/Mt_b) \int_0^{Mt_b} |S(t)|^2 dt} \quad (28)$$

In the remaining part of this article, an approximation will be made by which only  $M \times N \times l$  equidistant samples of  $S(t)$  will be considered, where  $l$  is an integer that is larger than or equal to 1; observe that the signal is  $l$ -times over sampled in the time domain. For each time interval  $[(m-1)t_b, mt_b]$ , these signal samples are represented as a vector  $\mathbf{S}^m = [s_0^m, s_1^m, \dots, s_{Nl-1}^m]$  and obtained as

$$s_k^m = S\left((m-1)t_b + \frac{k}{Nl}t_b\right) = \sum_{n=1}^N a_{n,m} e^{j2\pi(n-1)k/(Nl)}, \quad (29)$$

$$k = 0, 1, \dots, Nl - 1$$

It can be seen that the vector  $\mathbf{S}^m$  can be interpreted as the inverse discrete Fourier transform (IDFT) of the code block  $a_{n,m} (1 \leq n \leq N)$  with  $(l-1)N$  zero padding. It is well known that the PAPR of a continuous-time signal cannot be precisely obtained using its samples. However, it is shown in [29] that  $l \geq 4$  can provide sufficiently accurate results of the PAPR. The PAPR computed from samples of the  $l$ -times over sampled time-domain signal is given by

$$\text{PAPR} = \frac{\max_{0 \leq k < MNl-1} |s_k|^2}{E\{|s_k|^2\}} \quad (30)$$

where  $E\{\cdot\}$  denotes expectation.

Now, before the presentation of the algorithm, in the following paragraph, a method is introduced by which the sidelobe level in ACF can be reduced without any change in the PAPR.

Again, consider the pulsed signal of (1). It can be shown that this signal is constructed of components  $[s_m(t)]$  that are defined as follows

$$s_m(t) = \sum_{n=1}^N a_{n,m} \exp\left[j\frac{2\pi(n-1)t}{t_b}\right] P(t), \quad (31)$$

$$1 \leq m \leq M$$

where  $P(t)$  is the previously defined pulse and, thus, outside the interval  $[0, t_b]$ ,  $s_m(t)$  is equal to zero. By this definition,  $S(t)$  can be written as

$$S(t) = \sum_{m=1}^M s_m(t - (m-1)t_b) \quad (32)$$

Now, the time-domain circular shifted version of  $s_m(t)$  for any arbitrary  $d_m$  is defined as

$$\bar{s}_m(t) = s_m((t - d_m) \bmod t_b), \quad 1 \leq m \leq M, \quad (33)$$

$$0 \leq t \leq t_b$$

Here,  $\bar{s}_m(t)$  is also zero outside the interval  $[0, t_b]$ . Again by  $\bar{s}_m(t)$  of (33),  $\bar{S}(t)$  can be defined as

$$\bar{S}(t) = \sum_{m=1}^M \bar{s}_m(t - (m-1)t_b) \quad (34)$$

It is clear that each  $\bar{s}_m(t)$  has the same PAPR as  $s_m(t)$ . Consequently,  $S(t)$  and  $\bar{S}(t)$  have equal PAPR for any arbitrary set of  $\{d_m\}_{m=1}^M$ . However, these two signals  $[S(t)$  and  $\bar{S}(t)]$  have different SLLs in their ACF and by intelligent choice of the set  $\{d_m\}_{m=1}^M$ ,  $\bar{S}(t)$  can achieve a lower SLL than that of  $S(t)$ . Now we want to show the relation between  $S(t)$  and  $\bar{S}(t)$  in another manner. From (31)–(34), it can be deduced that

$$\begin{aligned} \bar{S}(t) &= \sum_{n=1}^N \sum_{m=1}^M a_{n,m} \exp\left[j\frac{2\pi(n-1)(t - d_m)}{t_b}\right] \\ &\times P(t - (m-1)t_b) \\ &= \sum_{n=1}^N \sum_{m=1}^M a_{n,m} \exp\left(-j2\pi(n-1)\frac{d_m}{t_b}\right) \\ &\times \exp\left(j2\pi(n-1)\frac{t}{t_b}\right) P(t - (m-1)t_b) \end{aligned} \quad (35)$$

Now, if we define

$$\lambda_m = -\frac{d_m}{t_b} \quad (36)$$

(35) can be rewritten as

$$\bar{S}(t) = \sum_{n=1}^N \sum_{m=1}^M \bar{a}_{n,m} \exp\left(j2\pi(n-1)\frac{t}{t_b}\right) P(t - (m-1)t_b) \quad (37)$$

In the above equation, the following definition is used

$$\bar{a}_{n,m} = a_{n,m} \exp(j2\pi(n-1)\lambda_m) \quad (38)$$

Hence, for any arbitrary set of  $(\lambda_1, \lambda_2, \dots, \lambda_M)$ , if a pulsed OFDM signal  $\bar{S}(t)$  with a corresponding  $N \times M$  code of  $[\bar{a}_{n,m}]_{N \times M}$  is produced from  $S(t)$  with a corresponding code of  $[a_{n,m}]_{N \times M}$  [where they are related by (38)], then the two signals  $S(t)$  and  $\bar{S}(t)$  will have the same PAPR; however, a suitable choice of  $(\lambda_1, \lambda_2, \dots, \lambda_M)$  can lead to a lower SLL for the ACF of  $\bar{S}(t)$  compared with that of  $S(t)$ .

Now, with this introduction, we are ready to present the PAPR reduction algorithm. First, using a proper search

method such as a genetic algorithm [30], we search for a vector  $(\lambda_1, \lambda_2, \dots, \lambda_M)_{\text{opt}}$  that results in the highest reduction of the SLL when we multiply  $\exp(j2\pi(n-1)\lambda_{m,\text{opt}})$  by the codes of the  $n$ th ( $n = 1, 2, \dots, N$ ) frequency relative to the  $m$ th interval. In Fig. 6, this procedure is shown. Hence, the obtained codes after this level are  $\bar{a}_{n,m;\text{opt}}$ , where

$$\bar{a}_{n,m;\text{opt}} = a_{n,m} \exp(j2\pi(n-1)\lambda_{m;\text{opt}}) \quad (39)$$

Thus, at the end of this step, a signal with the same PAPR but less ACF SLL than before is obtained. The next step is clipping. In this step, the signal is clipped with the threshold (Th) being a fraction of the maximum value of the signal [e.g. 0.95 of  $\max\{|S(t)|\}$ ], and the signal  $\tilde{S}(t)$  is constructed as follows

$$\tilde{S}(t) = \begin{cases} S(t), & |S(t)| < \text{Th} \\ \text{Th} \times \exp(j\text{Arg}(S(t))), & |S(t)| \geq \text{Th} \end{cases} \quad (40)$$

It is clear that this signal has a smaller maximum amplitude and less PAPR in comparison with  $S(t)$ . However,  $\tilde{S}(t)$  is not OFDM and an OFDM signal that is as similar to it as possible is required. To construct such a signal,  $M \times N \times l$  ( $l \geq 4$ ) uniform samples are taken from  $\tilde{S}(t)$  and are clustered into  $M$  sets, each containing  $N \times l$  samples. The DFT of each set is then computed and the first  $N$  transformed samples of each set are chosen as the frequency codes of the time interval related to that set. In this way, an  $N \times M$  code is produced whose time-domain equivalent signal  $[\tilde{S}(t)]$  is the most similar to  $\tilde{S}(t)$  in the sense of least-squares. This can be easily shown by the projection theorem for the Fourier series [31]. In brief, if the samples of  $\tilde{S}(t)$  are represented by  $\tilde{s}_k$ , where

$$\tilde{s}_k = \tilde{S}\left(\frac{kT}{M \times N \times l}\right), \quad k = 0, 1, \dots, M \times N \times l - 1, \quad T = Mt_b \quad (41)$$

the related code of the signal  $[\tilde{S}(t)]$  [the nearest OFDM signal

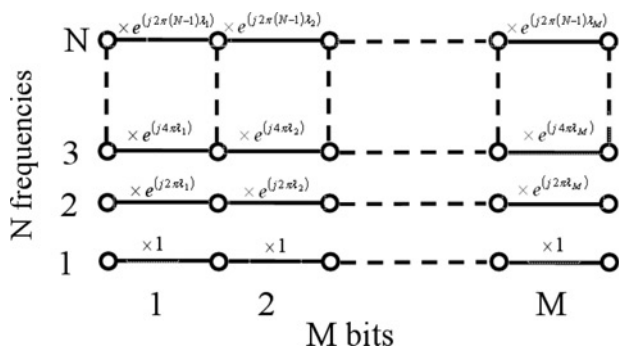


Figure 6 PAPR reduction process

to  $\tilde{S}(t)$ ] is obtained by the following expression

$$\tilde{a}_{nm} = \sum_{r=0}^{N \times l - 1} \tilde{s}_{(m-1) \times N \times l + r} \exp\left(-j2\pi \frac{r(n-1)}{N \times l}\right) \times (1 \leq n \leq N, 1 \leq m \leq M) \quad (42)$$

Thus, an OFDM signal is obtained having a PAPR less than that of  $S(t)$ , but its ACF SLL may be slightly higher than what it was before the clipping stage. Although the search algorithm found codes  $(\bar{a}_{n,m;\text{opt}})$  to optimise the SLL, that optimality was lost by clipping, which managed to reduce the PAPR; losing SLL optimality is the cost of PAPR reduction. However, if for some reason the SLL does not increase, no problem will occur, and actually the algorithm will work well.

In brief, the algorithm for the modification of codes to reduce the PAPR of an OFDM signal first multiplies each element of the code  $(a_{n,m})$  by  $\exp(j2\pi(n-1)\lambda_m)$  ( $n = 1, 2, \dots, N, m = 1, 2, \dots, M$ ), where the vector  $(\lambda_1, \lambda_2, \dots, \lambda_M)$  is found by a genetic algorithm and results in the highest reduction of the ACF SLL. The clipping level is continually repeated until the ACF SLL exceeds a previously selected threshold. Then, the  $N \times M$  OFDM signal nearest to the clipped signal is obtained by the explained method. In fact, the second and third steps of this algorithm reduce the PAPR at the expense of SLL growth, which has previously been compensated for in the first step without changing the PAPR. In other words, these three steps: (1) ACF SLL reduction by proper choice of  $(\lambda_1, \lambda_2, \dots, \lambda_M)$  (39), (2) clipping (40) and (3) finding the OFDM signal nearest to the clipped signal (42), are performed repeatedly until a desirable point in the algorithm trajectory appears.

## 6 Simulation results of code modification for PAPR reduction

In Sections 2 and 3, an algorithm was presented to design the pulsed OFDM signal with optimised AF and then, this algorithm was used in Section 4 to design a  $7 \times 7$  ( $M = 7, N = 7$ ) OFDM signal; and the resultant code was shown in Table 1. It was then shown how this method could achieve a code for which the AF SLL is low. However, as noted before, the designed OFDM signal has a large value of the PAPR and a rather high ACF SLL, which can be seen in Figs. 5a and 5b. In Section 5, the code-improving algorithm was presented to overcome this problem. Now, this algorithm is applied to refine the codes given in Table 1 and the resultant new code is presented in Table 2. The algorithmic process for PAPR reduction is depicted in Fig. 7. In the algorithmic trajectory, a point is obtained, which is marked by an asterisk, with PAPR = 1.7 and PSLL = 19.8 dB. In comparison with [8] in which the author could achieve PAPR = 2.93 and PSLL = 15 dB for



Table 2 Modified code parameters

Freq	Bit						
	1	2	3	4	5	6	7
(a) Magnitude							
1	2	2	2	2	2	3	7
2	3	2	1	1	1	2	6
3	3	3	8	7	8	8	4
4	9	9	3	0	2	3	3
5	8	9	2	0	2	2	4
6	2	3	8	7	8	8	2
7	2	1	1	1	1	1	4
(b) Phase (degree)							
1	111	168	−112	−65	−85	−156	131
2	−40	−93	102	−127	−62	75	−75
3	151	−44	80	−26	−113	−30	−54
4	−77	8	−125	−159	19	48	−90
5	−79	−107	94	79	34	−86	−133
6	64	−52	−115	−44	173	−9	−152
7	−121	10	−140	59	130	−100	−134

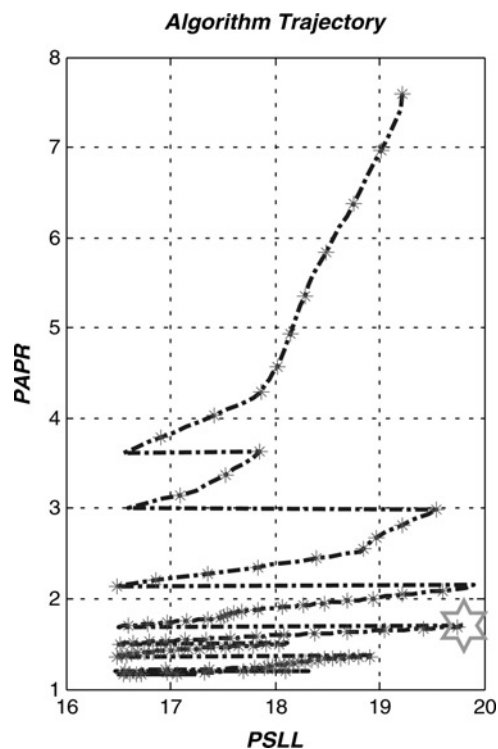


Figure 7 Algorithm trajectory for PAPR reduction

a pulsed OFDM signal with an even larger size of code ( $8 \times 8$ ) and without AF optimisation, the superiority of our proposed method is evident. Also, the AF, ACF and signal envelope are shown in Figs. 8, 9a and 9b, respectively. As can be seen, the proposed method could reduce the PAPR value from 7.7 to 1.7, which is precisely the value suitable for transmission. Actually, a PAPR lower than 4 is completely suitable [20] for communication applications, whereas, in radar applications, a PAPR lower than 2 is ideal [9]. Implicitly, the ACF SLL is decreased

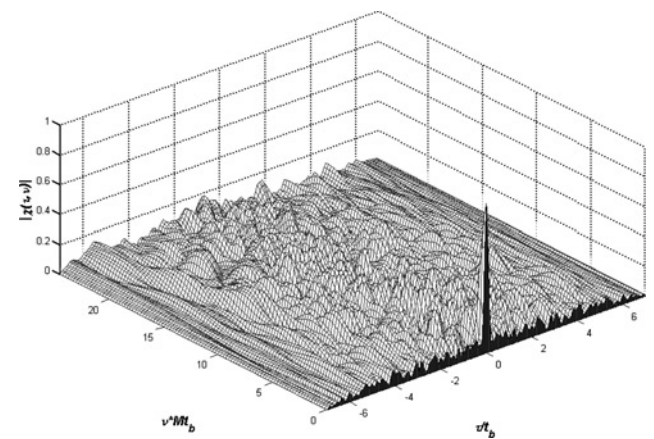
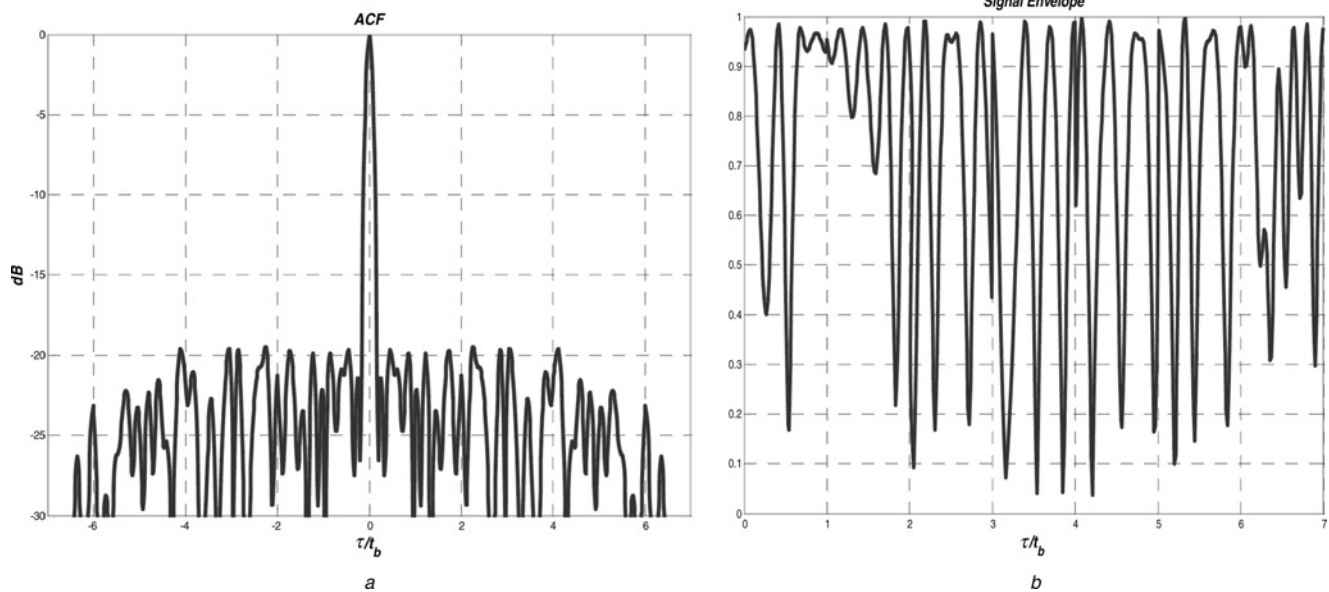


Figure 8 AF of modified OFDM signal



**Figure 9** ACF of the modified OFDM signal and real envelope of the modified OFDM signal

*a* ACF of the modified OFDM signal

*b* Real envelope of the modified OFDM signal

from  $-15$  dB to about  $-20$  dB (improvement of 5 dB) and the AF has a sidelobe level of less than  $-10$  dB. This means that the proposed algorithm could decrease the PAPR and the ACF SLL without destroying the AF.

## 7 Conclusion

In this paper, the least-squares method for AF synthesis was introduced. The method was then used to optimise the AF of an OFDM radar signal. It was shown that the method attempts to distribute the energy of sidelobes almost uniformly across the Doppler–delay plane. As a result, in contrast to previously devised methods, this method reduces the sidelobes not only along one axis, but also across the whole plane. An important practical point considered in this paper was the PAPR of the signal. To overcome this problem, an algorithm was proposed that could reduce the PAPR value by refining the codes without increasing the sidelobe level of the AF. Briefly, in this paper, we have presented a procedure by which one can design an OFDM signal with arbitrary numbers of frequency carriers and time intervals having optimised AF, low PAPR and good sidelobe level in the ACF.

## 8 References

- [1] SKOLNIK M.I.: 'Introduction to radar systems' (McGraw-Hill, International edn., 2000, 3rd edn.)
- [2] LEVANON N., MOZESON E.: 'Radar signals' (Wiley, Hoboken, NJ, 2004)
- [3] LEVANON N.: 'Multifrequency radar signals'. Records of the IEEE 2000 Int. Radar Conf., Alexandria, VA, 2000, pp. 683–688
- [4] COSTAS J.P.: 'A study of a class of detection waveforms having nearly ideal range–Doppler ambiguity properties', *Proc. IEEE*, 1984, **72**, (8), pp. 996–1009
- [5] SVERDLIK H.B., LEVANON N.: 'Family of multicarrier bi-phase radar signals represented by ternary arrays', *IEEE Trans. Aerosp. Electron. Syst.*, 2006, **42**, (3), pp. 933–953
- [6] LEVANON N.: 'Multifrequency complementary phase-coded radar signal', *IEE Proc., Radar Sonar Navig.*, 2000, **147**, (6), pp. 276–284
- [7] LEVANON N.: 'Train of diverse multifrequency radar pulses'. *Proc. IEEE Int. Radar Conf.*, 2001, Atlanta, GA, 2001, pp. 93–98
- [8] LEVANON N., MOZESON E.: 'Multicarrier radar signal-pulse train and CW', *IEEE Trans. Aerosp. Electron. Syst.*, 2002, **38**, (2), pp. 707–720
- [9] MOZESON E., LEVANON N.: 'Multicarrier radar signals with low peak-to-mean envelope power ratio', *IEE Proc., Radar Sonar Navig.*, 2003, **150**, (2), pp. 71–77
- [10] PRASAD N.N.S.R.K., SHAMEEM V., DESAI U.B., MERCHANT S.N.: 'Improvement in target detection performance of pulse coded Doppler radar based on multicarrier modulation with fast Fourier transform (FFT)', *IEE Proc., Radar Sonar Navig.*, 2004, **151**, (1), pp. 11–17

- [11] MOHSENI R., SHEIKHI A., MASNADI SHIRAZI M.A.: 'A new approach to compress multicarrier phase-coded signals'. Proc. 2008 IEEE Radar Conf., Rome, Italy, 26–30 May 2008, pp. 442–447
- [12] TSENG C.C., LIU C.L.: 'Complementary sets of sequences', *IEEE Trans. Inf. Theory*, 1972, **18**, (5), pp. 644–652
- [13] POPOVIC B.M.: 'Complementary sets based on sequences with ideal periodic autocorrelation', *Electron. Lett.*, 1990, **26**, (18), pp. 1428–1430
- [14] BLAU W.: 'Synthesis of ambiguity functions for prescribed responses', *IEEE Trans. Aerosp. Electron. Syst.*, 1967, **AES-3**, (4), pp. 621–627
- [15] GLADKOVA I., CHEBANOV D.: 'On the synthesis for a waveform having a nearly ideal ambiguity surface'. Int. Conf. Radar Systems, 2004
- [16] GLADKOVA I.: 'The Zak transform and a new approach to waveform design', PhD dissertation, City University of New York, 1998
- [17] WILCOX C.: 'The synthesis problem for radar ambiguity functions'. Tech. Summary Report No. 157, Mathematics Research Center, University of Wisconsin, Madison, Wisconsin, April 1960
- [18] SUSSMAN S.M.: 'Least-square synthesis of radar ambiguity functions', *IRE Trans. Inf. Theory*, 1962, **8**, pp. 246–254
- [19] MOHSENI R., SHEIKHI A., MASNADI SHIRAZI M.A.: 'Constant envelope OFDM signals for radar applications'. Proc. 2008 IEEE Radar Conf., Rome, Italy, 26–30 May 2008, pp. 453–457
- [20] HAN S.H., LEE J.H.: 'An overview of peak-to-average power ratio reduction techniques for multicarrier transmission', *IEEE Wirel. Commun.*, 2005, **12**, (2), pp. 56–65
- [21] SCHROEDER M.R.: 'Synthesis of low-peak factor signals and binary sequences with low autocorrelation', *IEEE Trans. Inf. Theory*, 1970, **16**, pp. 85–89
- [22] NEWMAN D.J.: 'An L extrema1 problem for polynomials', *Proc. Am. Math. Soc.*, 1965, **16**, pp. 1287–1290
- [23] NARAHASHI S., NOJIMA T.: 'New phasing scheme of  $N$  multiple carriers for reducing peak-to-average power ratio', *Electron. Lett.*, 1994, **30**, pp. 1382–1383
- [24] BOYD S.: 'Multi tone signals with low crest factor', *IEEE Trans. Circuits Syst.*, 1986, **33**, (10), pp. 1018–1022
- [25] VAN DER OUDERAA E., SCHOUKENS J., RENNEBOOG J.: 'Peak factor minimization, using time-frequency domain swapping algorithm', *IEEE Trans. Instrum. Meas.*, 1988, **37**, (1), pp. 144–147
- [26] VAN DER OUDERAA E., SCHOUKENS J., RENNEBOOG J.: 'Peak factor minimization of input and output signals of linear systems', *IEEE Trans. Instrum. Meas.*, 1988, **37**, (2), pp. 207–212
- [27] FRIESE M.: 'Multitone signals with low crest factor', *IEEE Trans. Commun.*, 1997, **45**, (10), pp. 1338–1344
- [28] VAN DEN BOS A.: 'A new method for synthesis of low-peak-factor signals', *IEEE Trans. Acoust. Speech Signal Process.*, 1987, **35**, (1), pp. 120–122
- [29] TELLAMBURA C.: 'Computation of the continuous-TimePAR of an OFDM signal with BPSK sub carriers', *IEEE Commun. Lett.*, 2001, **5**, (5), pp. 185–87
- [30] HAUPT R.L., HAUPT S.E.: 'Practical genetic algorithm' (Wiley, 2004)
- [31] BROWDER A.: 'Mathematical analysis: an introduction' (Springer, 2001)